A Numerical Study of Solitons Stability in 1D Bose-Einstein Condensates Using Split-Step Fourier Method

1 Introduction

In quantum systems, wave packets tend to spread out over time due to dispersion. For example, a particle in a box might be described by a Gaussian wave packet, which starts locally and gradually becomes broader as it evolves. In contrast to typical wave packets, a soliton is a stable, localized dip that maintains its shape while moving through space, even after interacting with other solitons[1]. Imagine a wave that travels across the ocean without losing its shape- no spreading, no fading, just a single, stable ripple moving undisturbed - this is the essence of a soliton, a unique non-dispersive wave packet. In quantum mechanics, solitons are typically characterized by a dip or a peak in probability density.

One important setting where solitons appear is Bose-Einstein condensates (BECs). BEC is a unique state of matter that forms when a larger number of bosons are cooled to a temperature very close to absolute zero[2]. At these temperatures, all particles collapse into a ground state, behaving collectively like a "single" particle. Unlike the Schrödinger equation (Equation (2.1.1)) that models a single-particle quantum system with no interactions, a more realistic depiction of BECs includes interatomic interactions. These interactions are typically attractive or repulsive, depending on the specific atom. When interatomic interactions are included, the governing equation becomes the Gross-Pitaevskii Equation (GPE), a nonlinear version of the Schrödinger, describing when describing dynamics of solitons.

The paper presents a numerical study of soliton dynamics in one-dimensional BECs, focusing on whether solitons maintain their shape after interacting with each other. We use a computational approach called the Split-Step Fourier Method (SSFM) to simulate soliton collision and evaluate their probability density function as a function of position and time.

2 Background Knowledge

2.1 Schrödinger Equation and Perturbations

The Schrödinger equation is a foundational differential equation in quantum mechanics, describing how the quantum states of a non-relativistic system evolve over time. The Schrödinger equation is given by Equation (2.1.1), where $\vec{r}$ is the position vector, ∇^2 is the Laplacian, and $\Psi(\vec{r},t)$ is the wave function.

$$\left(-\frac{\hbar^2}{2m}\nabla^2+V(\vec{r},t)\right)\Psi(\vec{r},t)=i\hbar\frac{\partial\Psi}{\partial t}(\vec{r},t) \tag{2.1.1}$$

The energy-eigenvalue equation of Equation (2.1.1) is given by Equation (2.1.2), where $\hat{H}$ is the Hamiltonian operator given by Equation (2.1.3).

$$\hat{H}\psi(\vec{r},t) = i\hbar\frac{\partial\Psi}{\partial t}(\vec{r},t) \tag{2.1.2}$$

The operator $\hat{H}$ consists of two parts: kinetic and potential energies operators.

$$\hat{H} = \underbrace{-\frac{\hbar^2}{2m}\nabla^2}_{\text{(kinetic)}} + \underbrace{V(x)}_{\text{(potential)}} \tag{2.1.3}$$

In many systems, the Schrödinger equation the Schrödinger equation successfully describes a known potential. These systems have well-defined eigenstates, each with predictable time evolution. In such idealized cases, no external force or internal interactions exist to complicate the behavior. However, while the equation works well for a simple system, it becomes inadequate for more complex systems, such as BECs, where particle interactions become not negligible. Realistic systems often experience perturbations, a deviation caused by internal interactions between particles.

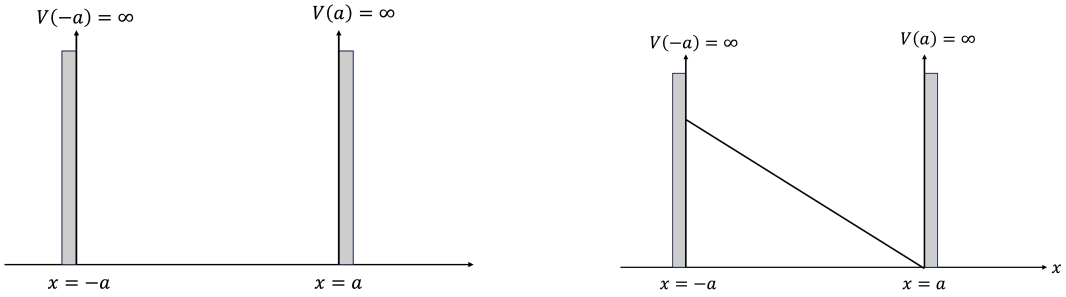

(a) A unperturbed infinite potential well with potential energy $V_0(x)$ and Hamiltonian $\hat{H}_0$

(b) A perturbed infinite potential with $V(x)$ and $\hat{H} = \hat{H}_0 + H'(x)$

Figure 1: A one-dimensional infinite potential well with width $2a$. (a) shows a well-defined, undisturbed system. (b) shows a disturbed system by introducing a linear potential $x - a$ inside the well, adding a new term $H'(x)$ to the Hamiltonian.

In simple terms, a perturbation refers to modifications to the system's Hamiltonian, typically modeled as an additional term in the potential energy. This is analogous to a well-tuned instrument (the unperturbed system) being gently nudged (the perturbation), producing a slightly altered but still recognizable tone. To illustrate this, consider a one-dimensional infinite potential well of width a and a well-defined potential energy Equation (2.1.4).

$$V_0(x) = \begin{cases} 0 & -a < x < a \\ \infty & \text{otherwise} \end{cases} \tag{2.1.4}$$

The corresponding unperturbed Hamiltonian $\hat{H}_0$ is:

$$\hat{H}_0 = -\frac{\hbar^2}{2m}\frac{d}{dx^2} + V_0(x) \quad -a < x < a \tag{2.1.5}$$

Introducing a perturbation by a linear potential x inside the well, the potential energy $V(x)$ is:

$$V(x) = \begin{cases} x - a & -a < x < a \\ \infty & \text{otherwise} \end{cases} \tag{2.1.6}$$

Accordingly, the perturbed Hamiltonian is given by Equation (2.1.7)

$$\hat{H} = \hat{H}_0 + \hat{H}', \quad \text{where } \hat{H} = x - a \tag{2.1.7}$$

The perturbation alters the system's energy operator and dynamics. The idea of perturbation is essential in studying quantum systems, such as BECs, where internal atomic interactions introduce deviations from the ideal non-interacting behavior.

2.2 BECs and Solitons

A BEC is a quantum phenomenon in which a large number of bosons simultaneously occupy the ground state of a system when near absolute zero [2], and a boson is a particle with integral spins, such as photon. At such low temperatures, atoms move very slowly relative to one another and begin to behave indistinguishably. At this stage, atoms cluster together and act as if they are a single atom. In idealized models of BECs, interatomic interactions between bosons are neglected, treating it as a non-interacting system modeled. However, realistic BECs involve interactions, introducing perturbations. These interactions give rise to solitons, a frequently observed disturbance in BECs.

A soliton is a localized, stable disturbance in the probability density. Unlike many wave packets that disperse over time, it moves with a constant velocity and preserves its shapes, even after colliding with other solitons. Solitons re-emerge with the same shape and velocities after a collision. The non-disperse nature of solitons is illustrated by Figure 2, showing two localized dips moving toward each other at the same speed. As shown by the figure, solitons maintain the same shape and depth in probability density as time evolves from $t[\tau] = 0$ to $t[\tau] = 15$.

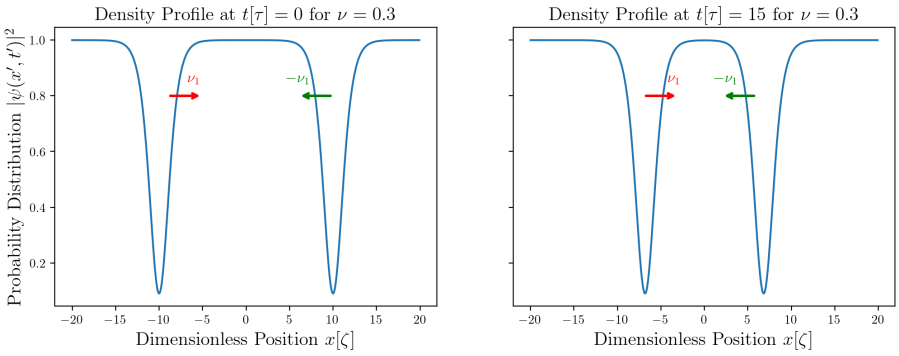

Figure 2: Probability density of two solitons for a head-on collision with a speed of $\nu = 0.3$. The profile is simulated using Equation (2.3.7) at $t[\tau] = 0$ and $t[\tau] = 15$ for $\nu = 0.3$

While there are several types of solitons, the paper focuses on dark and grey solitons. A dark soliton is a localized dip in the probability density of a BEC. The stationary or slow-moving solitons are often characterized by a probability density of zero at the center [3]. These solitons

occur in repulsive interactions. Grey solitons are moving darks, exhibiting a non-zero speed and a shallower dip in probability density.

2.3 The Gross Pitaevskii Equation

To describe the behavior of interacting BECs more accurately, we modify the Schrödinger equation to include a nonlinear term $g|\psi|^2\psi$, leading to the Gross-Pitaevskii Equation (GPE) by Equation (2.3.1), where m is the mass of bosons, $V(\vec{r})$ is the potential energy, and g is a dimensionless parameter measuring the strength interatomic interaction [1]. The additional term $g|\psi|^2\psi$ accounts for interatomic interactions, such as solitons in a system of identical bosons in the ground state. If $g > 0$, it represents repulsive interactions. If $g < 0$, the interaction is attractive.

$$i\hbar\frac{\partial\Psi(\vec{r},t)}{\partial t} = \left(-\frac{\hbar^2}{2m}\nabla^2+V(\vec{r}) + g|\Psi(\vec{r},t)|^2\right)\Psi(\vec{r},t) \tag{2.3.1}$$

In the paper, we consider the one-dimensional case with $V(x) = 0$ $g = 1$ for repulsive interaction, simplifying Equation (2.3.1) to Equation (2.3.2). The paper simulates a **symmetric head-on collision between two solitons**, meaning that the initial positions of two solitons are symmetric about the x axis and velocities are equal in magnitude but opposite in direction.

$$i\hbar\frac{\partial\Psi(x,t)}{\partial t} = \left(-\frac{\hbar^2}{2m} + g|\Psi(x,t)|^2\right)\Psi(x,t) \tag{2.3.2}$$

To reduce the number of parameters, the paper non-dimensionalize Equation (2.3.2) using three key concepts: (1) the Bogoliubov speed c_s, (2) background density ρ_0, and (3) the healing length ζ. The Bogoliubov speed c_s by Equation (2.3.3) is the speed of perturbations propagating through condensates, where ρ_0 is the background probability density when BEC is far away from any disturbances. That is the probability density when no perturbation, soliton, is present.

$$c_s = \sqrt{\frac{g\rho_0}{m}} \tag{2.3.3}$$

The healing width ζ is the minimum distance over which the BEC can "heal" (smooth out) a local disturbance and restore to ρ_0, defined by Equation (2.3.4).

$$\zeta = \frac{\hbar}{\sqrt{mg/\rho_0}} \tag{2.3.4}$$

For instance, a dark solitons' density profile transitions from ρ_0 to a dip in a wave function. The healing length ζ defines how quickly the BEC fills in the dip and returns to its undisturbed background density ρ_0. The paper defines the following quantities by Equation (2.3.5).

$$\psi' = \frac{\psi}{\sqrt{\rho_0}} \quad x' = \frac{x}{\zeta} \quad t' = \frac{t}{\tau} \quad \tau = \frac{\zeta}{c_s} \tag{2.3.5}$$

Differentiating and substituting dimensionless quantities, the dimensionless GPE is given by Equation (2.3.6) [4](see Appendix A for details).

$$i\frac{\partial\psi'(x',t')}{\partial t'} = \underbrace{-\frac{1}{2}\frac{\partial^2\psi(x',t')}{\partial x'^2}}_{\text{linear}} + \underbrace{|\psi'(x',t')|^2\ \psi'(x',t')}_{\text{nonlinear}} \tag{2.3.6}$$

For one dimensional BEC with $g = 1$, the GPE admits solutions given by Equation (2.3.7) [1], where ν is the dimensionless speed by Equation (2.3.8), γ is the Lorentz factor defined by Equation (2.3.9), and x_0' is the absolute value of the initial position of two solitons.

$$\psi'(x',t') = \left[i\nu + \frac{1}{\gamma}\tanh\left(\frac{x'-x_0'-\nu t}{\gamma}\right)\right]e^{it} \tag{2.3.7}$$

$$\nu = \frac{v_s}{c_s} \tag{2.3.8}$$

$$\gamma = \sqrt{1-\frac{v^2}{c_s^2}} = \sqrt{1-\nu^2} \tag{2.3.9}$$

Note that notations of $x[\zeta]$ and $t[\tau]$ in figures in Section 3 are the same as x' and t'. The use $x[\zeta]$ and $t[\tau]$ only indicate that position and time are scaled by ζ and τ for non-dimensionlization.

3 1D Soliton Simulation as An Example

3.1 Simulation Set-Up

To study soliton behavior in one-dimensional BECs, we simulate using the split-step Fourier method (SSFM), alternatively evolving the wave function under linear and nonlinear terms [5]. SSFM method numerically evolves the dimensionless GPE equation(Equation (2.3.6)) over time [6]. The key quantity evaluated is the probability density $|\psi'(x',t')|^2$, calculated across various points in space and time to visualize the solitons' motion.

To model the system, the paper defines a finite and symmetric spatial domain from $[-x', x'] = [-20, 20]$, mimicking the infinite potential well introduced earlier(Figure 1). Within the domain, the simulation assumes a background density of $\rho_0 = 1$, meaning that the probability of finding a particle within $-20 < x' < 20$ when no soliton is present is $\rho = 1$. When solitons are present, the wave function is given by Equation (2.3.7) and zero elsewhere both the disturbance is and is not present. Thus

$$\psi(x',t') = \begin{cases} \left(i\nu + \frac{1}{\gamma}\tanh\left(\frac{x'-x_0'-\nu t}{\gamma}\right)\right)e^{it} & -20 < x' < 20 \\ 0 \quad \text{elsewhere} \end{cases} \tag{3.1.1}$$

Although the wave function is not normalized initially, working with a finite domain allows normalization. The wave function can be rescaled using the total area under the probability density curve.

$$\int_{-a}^{a} |\psi'(x',t')|^2 dx = A, \quad \text{where A is the area under the curve} \tag{3.1.2}$$

The assumption of $\rho_0 = 1$ implies in the absence of any soliton, the probability of finding a particle at any point within $[-20, 20]$ is equal. This might seem unrealistic, but setting ρ_1 is a common simplification and is often used as a natural unit that makes calculating easier while preserving the qualitative features of soliton dynamics [4].

$$\psi'_{\text{normalized}}(x',t') = \frac{1}{\sqrt{A}}\psi'(x',t') \tag{3.1.3}$$

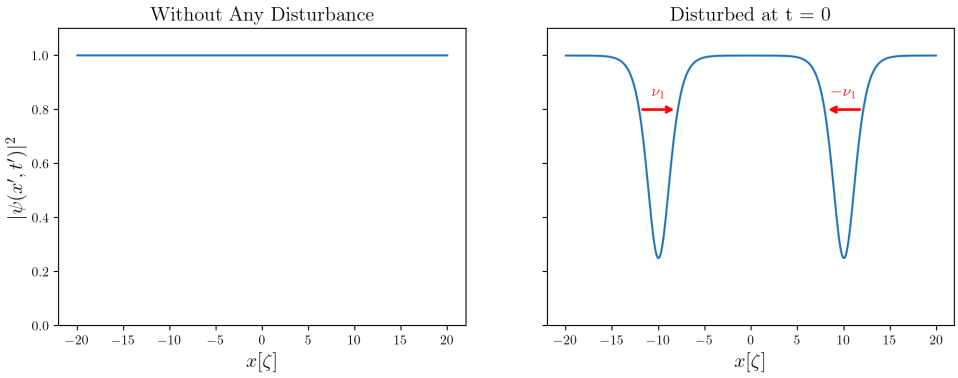

Figure 3: The left subplot shows a background density of $\rho_0 = 1$ when no soliton is present. The right subplot shows two symmetric, localized disturbances by two solitons, moving with an equal and opposite velocity($\nu_1 = -\nu_2$) for a head-on collision. Note that $x[\zeta]$ and $t[\tau]$ are same as x' and t'.

Figure 3 more clearly illustrates the set-up. The left subplot shows a uniform density profile with $\rho_0 = 1$, indicating an equal likelihood of finding a particle when no soliton is present. In contrast, the right subplot displays the system when disturbances are introduced. Two localized dips appear, moving toward each other with an equal and opposite velocity $\nu_1 = -\nu_2$. Each dip represents a soliton, disturbing the background density that reduces the probability density at that position. These localized dips signify disturbances in background density ρ_0. To study soliton dynamics, we simulate a head-on collision between two solitons. The solitons begin at symmetric initial positions $x' = 10$ and $x' = -10$.

3.2 Re-emergence of Dips

To further investigate the shape-preserving nature of solitons, we simulate a symmetric head-on collision where the initial velocities where $\nu_1 = -\nu_2$. In one simulation, we choose $\nu_1 = -\nu_2 = 0.5$ and plot a sequence of probability density as a function of x' over time, shown by Figure 4 [7]. Figure 4 shows the three stages before, during, and after the collision.

The first row corresponds to before collision. Before the collision, the two solitons are well-separated, with clearly visible and symmetric dips. Both solitons have an identical shape (same dip depth) and equal speeds in opposite directions. This corresponds to the top of the plot when $t[\tau] = 0$.

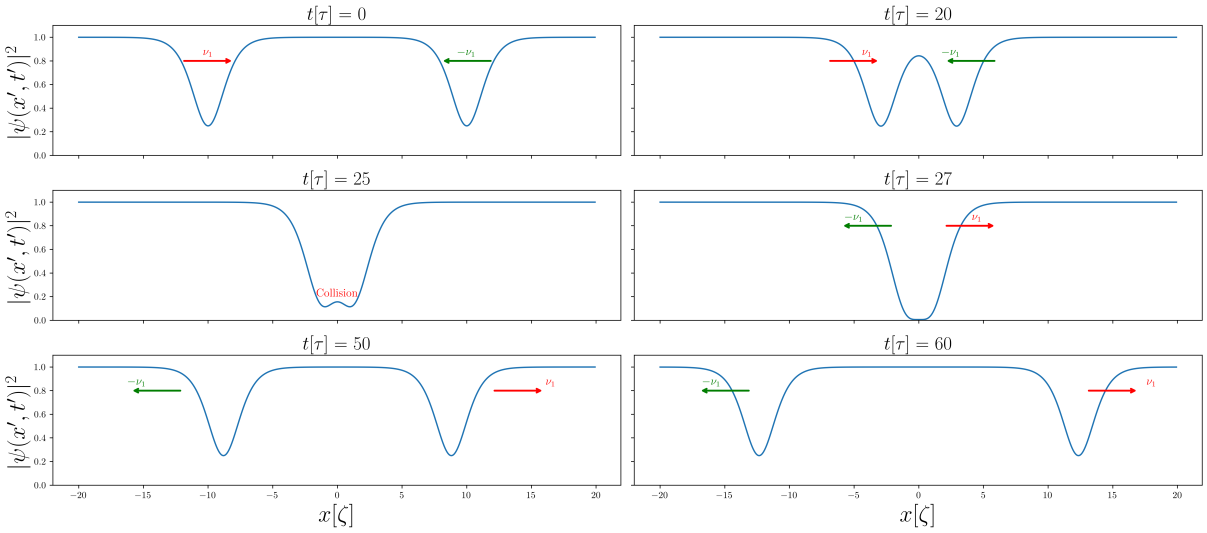

Figure 4: Evolution of probability density $|\psi(x', t')|^2$ of two solitons when $\nu = 0.5$. The first row for before the collision, second row for during the collision, and last row for after the collision.

As time progresses, the solitons approach each other and eventually collide. During this stage, atomic interactions become dominant, as represented by the coupling term $|\psi'|^2\psi'$ in Equation (2.3.6), and dips start to overlap. When solitons start to overlap, their wave functions interfere destructively, resulting in a temporary decrease in probability density. This is evident in Figure 4, where the $|\psi(x', t')|^2$ drops from approximately$|\psi(x', 25)|^2 = 0.2$ at $t' = 25$ to about $|\psi(x', 27')|^2 = 0.1$ at $t' = 27$. After the collision, two solitons separate and continue to propagate, as shown by (c) of Figure 4. Interestingly, each dip retain its the original same shape and velocity as before. The simulation shown in Figure 4 confirms the shape-preserving nature of solitons: dips maintain the same shape and depth after interaction, despite undergoing nonlinear interference during the collision.

3.3 Density Profile and Preservation of Shape

To further explore solitons' stability, we examine their evolution for different velocity ν. Figure 5 shows a series $|\psi'(x', t')|^2$ vs x' contour plots, illustrating the evolution of soliton density profiles for various ν [7]. They might look complicated, but do not worry. The contour map means that the graph shows information about x', t', and $|\psi(x', t')|^2$ simultaneously at each (x', t') position. The horizontal axis represents position x', while the vertical axis represents time t', same as $x[\zeta]$ and $t[\tau]$ in the figure. The color bar on the side shows the value of probability density $|\psi(x', t')|^2$ each color corresponds. A brighter color indicates a higher probability density value for a shallower dip, and a darker color signifies a deeper dip for a smaller $|\psi(x', t')|^2$ value. Each contour plot shows two beams representing the trajectories of the two solitons over time, where the probability density value at (x', t') at each time is indicated by its color.

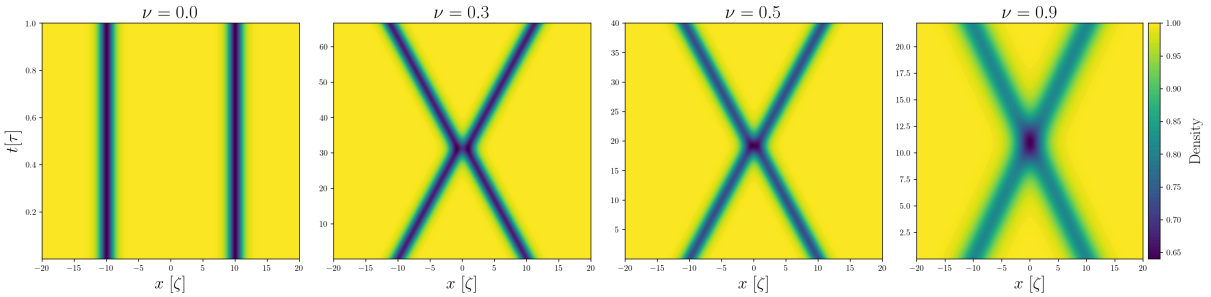

Figure 5: The density profile of simulated solitons at various velocity ν, each with initial positions $x' = 10$ and $x' = -10$. The vertical axis shows the time required to travel 20 units. As ν increases, time decreases and probability density increases, indicated by brighter colors.

Figure 5 shows the evolution of $|\psi(x', t')|^2$ over time. If a soliton's' shape changes, meaning that the value of $|\psi(x', t')|^2$ changes, a change in color will be indicated. Figure 5 shows consistent coloring in contour plots, showing that both ($\nu = 0$) and grey($\nu > 0$) solitons retain their shape and dip depth after collision. In addition, the slope of x' and t indicates velocity. In Figure 4, beams have a constant slope throughout the simulation, showing that velocity is unchanged after the collision. The perseverance of shape and velocity is consistent with the theoretical prediction, illustrating soliton stability in one-dimension.

3.3.1 Black Soliton for $\nu = 0$

Equation (2.3.7) shows the density profile of a black soliton when $\nu = 0$. he presence of two symmetric density dips centered around $x' = 0$ validates the simulation's set up for a symmetric head-on collision. As seen in the figure, the two beams are vertically aligned at $x = -10$ and $x = 10$ throughout the simulation with no change in position, indicating that the solitons are stationary. This consistent position of solitons shows that no motion has occurred. Moreover, the absence of an intersection between the two beams further confirms that no interaction has taken place—the solitons remain at rest and non-interacting.

The dark soliton is a special case as it shows the strongest possible suppression in probability density. When $\nu = 0$, Equation (2.3.7) simplifies to Equation (3.3.1.1).

$$|\psi'_{\nu=0}(x, t)|^2 = \tanh(x' - x'_0) \tag{3.3.1.1}$$

The equation describes the deepest dip, with probability density dropping to zero at the center $x' = x'_0$.

3.3.2 Velocity Limit $\nu \to 1$

As ν increases, we observe two patterns: (1) trajectories become blurred(wider) and brighter, indicating higher $|\psi|^2$ values, and (2) a darkened region where the two trajectories intersect.

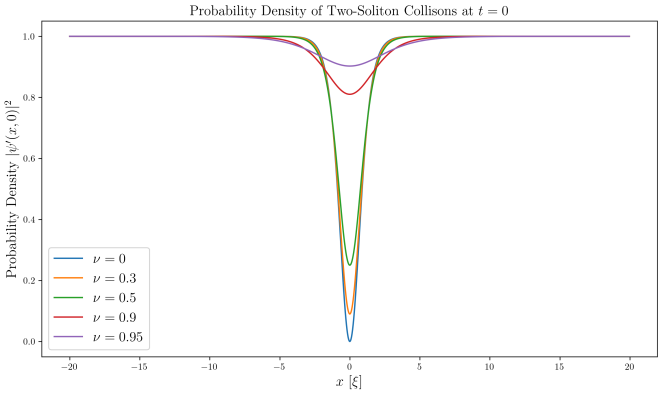

Figure 6: Dips of solitons at various ν at $t' = 0$, showing that decreases in depth as ν increase.

The first observation suggests that dips become shallower and more spatially dispersed. Since $|\psi'(x,t)|^2$ represents local probability density, a shallower dip corresponds to a higher $|\psi'(x',t')|^2$ value. The increase in brightness in Figure 5 is a direct visual manifestation of these effects and is more directly shown by Figure 6. The result is consistent with Equation (2.3.7). When $\nu \to 1$, the Lorentz factor approaches ∞.

$$\lim_{\nu \to 1} \gamma = \lim_{\nu \to 1} \frac{1}{\sqrt{1-\nu^2}} \to \infty \tag{3.3.2.1}$$

and $|\psi'(x,t)|^2 \to 1$, same as the undisturbed background density of $\rho_0 = 1$.

$$\lim_{\nu \to 1} \psi'(x',t') \approx i\nu e^{it} \to |\psi'(x,t)|^2 = (i\nu e^{it})(-i\nu e^{-it}) = \nu^2 \approx 1 \tag{3.3.2.2}$$

As a result, solitons' tanh-shaped dip flattens out, effectively losing its dip. To physically understand this, recall that ν is defined as the ratio of soliton speed to the speed of sound in the condensate. When ν is small, solitons are nearly stationary, so it takes longer for disturbances to move away from the system. Consequentially, solitons continuously perturb the system, maintaining deep, localized dip. In contrast, for larger ν, the soliton moves faster through the system, spending less time in any region. The reduced time results in less disturbance and thus broader, shallower dips in the probability density. This is also evident from the time scales in Figure 5. As ν increases from $\nu = 3$ to $\nu = 9$, the time required to travel a distance of $x' = 20$ decreases from $t' = 70$ to $t' = 23$.

For the second observation, at the points where two trajectories intersect, the region where a collision occurs, a darker point is shown. The effect is more clearly observed as $\nu \to 1$. The darkening reflects a stronger interference between solitons when velocity increases, meaning that wave functions overlap more and become less distinguishable during collision. As the two wave functions, a greater suppression in probability density is produced, causing a smaller probability density value that is signified by a darker color.

4 Application

The paper simulated symmetric head-on collisions of two solitons using SSFM, confirming their ability to preserve shape and velocity after collisions. While the paper focuses on matter-wave solitons in BECs, the property has important implications in other physical systems, especially in quantum communication.

One essential application of solitons is optical fiber communication, where light pulses are transmitted through fiber to carry information [8]. One challenge in long-distance communication is dispersion: different frequency components of a light pulse travel at different speeds, causing the pulse to spread. The degradation leads to signal distortion and loss of information. Solitons, as a non-disperse wave packet, provide a possible solution[9]. Light pulses propagating through fibers are described by the GPE. Just like solitons in BECs, solitons in fiber counter-dispersions by their non-linear behavior, result in a stable, shape-preserving pulse that can travel long distances without distortion.

The shape-preserving behavior is crucial in fiber optics. Shape preservation ensures each pulse carries its encoded information is transmitted without distortions, reducing the need for signal regeneration. Moreover, because solitons reemerge with a preserved shape and velocity after an interaction, multiple soliton pulses can coexist in the same fiber without significant distortions. This enables multiplexing, meaning that a huge amount of pulses can be transmitted simultaneously without losing information Lastly, the non-dispersive nature of solitons allows them to be spaced closely along the fiber without overlapping. This tremendously improves data transmission efficiency. Today in quantum communication, soliton has been exploited to study many important practical problems. It remains one of the most active research due to its considerable applications in information and communication technology.

5 Conclusion

The paper presents a numerical study of soliton in one-dimensional BECs using SSFM. By simulating head-on symmetric collisions, we demonstrate that solitons maintain their shape and velocity after colliding, as shown by the preservation of density throughout the simulation. This confirms the stability of solitons in 1D BECs, driven by the balance between dispersive spreading and compressed governed by the GPE. The result does not only validate theoretical prediction but also highlights potential applications of solitons, particularly in quantum communication systems using optical fibers. Solitons' ability to propagate without dispersion and distortion them ideal candidates for long-distance data transmission. Ultimately, the stability of solitons in one dimension shows the powerful impact of quantum mechanics.

Bibliography

[1] R. BALAKRISHNAN and I. I. SATIJA, "Solitons in Bose–Einstein Condensates," *Pramana*, vol. 77, no. 5, pp. 929–947, Oct. 2011, doi: 10.1007/s12043-011-0187-z.

[2] M. Schwartz, "Harvard." [Online]. Available: https://scholar.harvard.edu/files/schwartz/files/12-bec.pdf

[3] S. Yang *et al.*, "Recent advances and challenges on dark solitons in fiber lasers," *Optics & Laser Technology*, vol. 152, p. 108116, 2022, doi: https://doi.org/10.1016/j.optlastec.2022.108116.

[4] S. Komineas, "UOC." [Online]. Available: http://users.math.uoc.gr/~komineas/Educational/MathModel/Modeling01_calculusOfVariations.pdf

[5] J. Javanainen and J. Ruostekoski, "Symbolic calculation in development of algorithms: split-step methods for the Gross–Pitaevskii equation," *Journal of Physics A: Mathematical and General*, vol. 39, no. 12, pp. L179–L184, Mar. 2006, doi: 10.1088/0305-4470/39/12/l02.

[6] T. Buss, J. Traub, and J. Gutekunst, "Thorstenbuss/CQD: The gross-pitaevskii equation (GPE): Dynamics of solitons and vortices." [Online]. Available: https://github.com/ThorstenBuss/CQD

[7] A. Bradley, [Online]. Available: https://ashtonsbradley.github.io/FGPEexamples.jl/html/2dharmonic.html

[8] Person, "What are fiber optics and how do they work?." [Online]. Available: https://www.coherent.com/news/glossary/optical-fibers

[9] S. Manukure and T. Booker, "A short overview of solitons and applications," *Partial Differential Equations in Applied Mathematics*, vol. 4, p. 100140, 2021, doi: https://doi.org/10.1016/j.padiff.2021.100140.

6 Acknowledgement

I would like to thank Youtube for teaching the basis of solitons, nonlinear Schrödinger equation, and cortices (though I did not get a chance to talk about it). I would also like to acknowledge platforms such as APS and IOP that allows me to download essays for FREE. I would like to thank [6] for providing codes for simulating GPE in python, the only programming language I am familiar with. Without them, it is impossible for me to come up with the topic and finish the term paper. . I want to acknowledge my peer for letting me know that the term paper needs to be DOUBLE SPACED. Thank you! I would also acknowledge my peer for peer review, although who that person was. The feedback was very detailed and helpful. Finally, I would like you thank Prof Breznay and Gerbode for providing feedbacks.

A Appendix

Substitute into Equation (2.3.1)

$$\frac{\partial\psi}{\partial t} = \frac{\partial\psi}{\partial t'}\frac{dt'}{dt} = \frac{\sqrt{\rho_0}}{\tau}\frac{\partial\psi'}{\partial t'} = \sqrt{\rho_0}\frac{g\rho_0}{\hbar}\frac{\partial\psi}{\partial t'} = \frac{g\rho_0^{3/2}}{\hbar}\frac{\partial\psi}{\partial t} \tag{1.1}$$

The special derivative is given by:

$$\frac{\partial\psi}{\partial x} = \frac{\partial\psi}{\partial x'\zeta} = \frac{\sqrt{\rho_0}}{\zeta}\frac{\partial\psi'}{\partial x'} \tag{1.2}$$

The second derivative is equal to:

$$\frac{\partial^2\psi}{\partial x^2} = \frac{\partial}{\partial x}\left(\frac{\sqrt{\rho_0}}{\zeta}\frac{\partial\psi'}{\partial x'}\right) = \frac{\sqrt{\rho_0}}{\zeta}\frac{\partial}{\partial x}\left(\frac{\partial\psi'}{\partial x'}\right) = \frac{\sqrt{\rho_0}}{\zeta}\frac{\partial}{\partial x'\zeta}\left(\frac{\partial\psi'}{\partial x'}\right) = \frac{\sqrt{\rho_0}}{\zeta^2}\frac{\partial^2\psi'}{\partial x'^2} \tag{1.3}$$

Substitute expressions, we get

$$\frac{\partial^2\psi}{\partial x^2} = \frac{\sqrt{\rho_0}2mg\rho_0}{\hbar^2}\frac{\partial^2\psi'}{\partial x'^2} = \frac{mg\rho_0^{3/2}}{\hbar^2}\frac{\partial^2\psi'}{\partial x'^2} \tag{1.4}$$

Then,

$$i\hbar\left(\frac{g\rho_0^{3/2}}{\hbar}\frac{\partial\psi'}{\partial t}\right) = -\frac{\hbar^2}{2m}\left(\frac{mgn_0^{3/2}}{\hbar^2}\frac{\partial^2\varphi}{\partial x'^2}\right) + gn_0^2|\psi'(x)|^2\ \sqrt{n_0}\psi' \tag{1.5}$$

Thus, the dimensionless GPE is:

$$i\frac{\partial\psi'}{\partial t} = -\frac{1}{2}\frac{\partial^2\psi'}{\partial x'^2} + |\psi'|^2\ \psi' \tag{1.6}$$